

Tracking unstable periodic orbits in nonstationary high-dimensional chaotic systems: Method and experiment

Bruce J. Gluckman* and Mark L. Spano

Naval Surface Warfare Center, White Oak Laboratory, Silver Spring, Maryland 20903

Weiming Yang and Mingzhou Ding

Program in Brain Sciences and Complex Systems, Center for Complex Systems and Department of Mathematical Sciences, Florida Atlantic University, Boca Raton, Florida 33431

Visarath In[†] and William L. Ditto

School of Physics, Georgia Institute of Technology, Atlanta, Georgia 30332

(Received 14 August 1996; revised manuscript received 17 December 1996)

We consider the adaptive control of chaos in nonstationary high-dimensional dynamical systems. In particular, we propose and experimentally implement a technique to stabilize and track unstable periodic orbits based on the use of time series. In our technique, the position of the periodic orbit and other parameters in the controller are continually updated from recent measurements of the system state and perturbation histories, while the environment, simulated by one or several of the system's parameters, drifts independent of the control algorithm. We demonstrate the effectiveness of the technique computationally for the Hénon map, a chemical reaction model, and a coupled driven Duffing oscillator, and experimentally for a magnetoelastic ribbon system. [S1063-651X(97)03405-3]

PACS number(s): 05.45.+b

I. INTRODUCTION

Recently, the theme of how to exploit the properties of chaos to do useful things has attracted a great deal of interest. One arena of this research is the development of chaos control techniques, in which small perturbations are applied to a nonlinear system to stabilize its naturally occurring chaotic dynamics into a periodic orbit [1,2]. It has been shown that by doing so one may improve the system's performance against general classes of criteria [3].

The basis for chaos control comes from the realization that a chaotic attractor has, embedded within it, an infinite number of unstable periodic orbits. The dynamics can be roughly approximated by a series of approaches to and subsequent divergences from these orbits. Regularization of the dynamics, or control, is enacted by perturbing the system so that it stays near one of these orbits. When viewed in the delay coordinate state space, the neighborhood of an unstable orbit can be separated into directions along which the dynamics either converge toward (stable) or diverge from (unstable) the orbit. A control law, which prescribes the perturbations, is designed such that the state space points are pushed into the subspace spanned by the stable directions. In the absence of the underlying equations of motion, the parameters needed for control are estimated from the time series. One salient feature of this control paradigm is that, since the target periodic orbit is part of the natural dynamics, the

control is often achieved with small perturbations.

A potential difficulty with a nonadaptive application of this type of technique to real physical problems is that systems' environments are rarely static. It is often the case that changing ambient physical conditions, entering the system as parameters, causes change in the dynamics in an irregular and unpredictable fashion. If small perturbation control is to be maintained, one must be able to continually update both the periodic orbit position and the other control parameters. Various scenarios have been considered [4] in which a momentary loss of control due to environmental variations and the lack of adaptive control leads to catastrophic system failures.

A further advantage is that tracking techniques can also be applied to extend the stable operation range of a system. In this case, parametric change may be done at the experimenter's discretion without loss of control.

In the present work we attempt to develop an adaptive control strategy to track an unstable periodic orbit under a changing environment. In particular, we are interested in doing so for high-dimensional systems where the periodic orbit cannot be effectively described by one stable and one unstable direction. Tracking an unstable periodic orbit in the context of chaos control was pioneered by Schwartz and Triandaf [5]. Additional work in this area can be found in [6,7].

The method we present in Sec. II has two components: a controller based on a general, high-dimensional control algorithm, assuming the use of time series [8], and a mechanism to update the controller, requiring no assumptions of how the environment varies with time. We demonstrate our technique's effectiveness in Sec. III by applying it computationally to a number of numerical examples, including the Hénon map, a chemical reaction model, and a coupled Duffing oscillator. We then implement the technique in Sec. IV in an

*Present address: Center for Neuroscience Research, Children's National Medical Center, Washington, DC 20010. Electronic address: Dgluckma@cnmc.org

[†]Present address: Naval Surface Warfare Center, Carterock Division, West Bethesda, MD 20817.

experimental physical system, a periodically driven, gravitationally buckled metallic ribbon, which exhibits chaotic behavior. Section V concludes this paper.

II. THE METHOD

Let a dynamical system be described by the following k -dimensional map on some Poincaré surface of section,

$$\mathbf{X}_{n+1} = \mathbf{F}(\mathbf{X}_n, p), \quad (1)$$

where $\mathbf{X} \in \mathbf{R}^k$ and p is the control parameter to be perturbed. Suppose that for $p = p^*$ Eq. (1) has a chaotic attractor. Without explicitly knowing \mathbf{F} , we base our analysis and control on a discretely measured time series $\{x_n\}$ of some scalar observable $x_n = h(\mathbf{X}_n)$. Using delay coordinates [9] we reconstruct the high-dimensional dynamics from $\{x_n\}$ via $\mathbf{z}_n = (z_n^{(1)}, z_n^{(2)}, \dots, z_n^{(m)})^T = (x_{n-m+1}, x_{n-m+2}, \dots, x_n)^T$, where m is the dimension of the reconstructed phase space and T denotes matrix transpose. For large enough m , \mathbf{z}_n is a global one-to-one representation of the variable \mathbf{X}_n on the original attractor. Since the control is done by changing the value of p according to a control law for every iteration of the map, the reconstructed discrete map for \mathbf{z}_n has the form

$$\mathbf{z}_{n+1} = \mathbf{G}(\mathbf{z}_n, p_{n-m+1}, p_{n-m+2}, \dots, p_n). \quad (2)$$

Here, \mathbf{G} generally depends on all the parameter variations effective during the time interval $n-m+1 \leq t \leq n$ spanned by the delay vector \mathbf{z}_n [10–12].

In the reconstructed phase space a fixed point for the nominal system (i.e., when $p = p^*$) is denoted by $\mathbf{z}^* = \mathbf{G}[\mathbf{z}^*(p^*), p^*, p^*, \dots, p^*]$. The Jacobian matrix for Eq. (2) is the following $m \times m$ matrix [11]:

$$\mathbf{A}_n = \mathbf{D}_{\mathbf{z}_n} \mathbf{G}(\mathbf{z}_n, p_{n-m+1}, p_{n-m+2}, \dots, p_n).$$

The set of m -dimensional column vectors,

$$\mathbf{B}_n^{(i)} = \mathbf{D}_{p_{n-i+1}} \mathbf{G}(\mathbf{z}_n, p_{n-m+1}, p_{n-m+2}, \dots, p_n),$$

for $i = 1, 2, \dots, m$ characterize the effect of the control parameter variations on the dynamics. Evaluating all the partial

derivatives at $\mathbf{z}_n = \mathbf{z}^*(p^*)$ and $p_{n-m+1} = p_{n-m+2} = \dots = p_n = p^*$, we obtain the linearized dynamics around the fixed point [11],

$$\begin{aligned} \delta \mathbf{z}_{n+1} = & \mathbf{A} \delta \mathbf{z}_n + \mathbf{B}^{(m)} \delta p_{n-m+1} \\ & + \mathbf{B}^{(m-1)} \delta p_{n-m+2} + \dots + \mathbf{B}^{(1)} \delta p_n, \end{aligned} \quad (3)$$

where $\delta \mathbf{z}_i = \mathbf{z}_i - \mathbf{z}^*$, $\delta p_i = p_i - p^*$, and we have dropped the reference to n for \mathbf{A} and \mathbf{B} since they are constant at the fixed point. We note that, due to the nature of the time series and delay coordinates used here, most of the entries in the above matrix and vectors are zero. Specifically, we have [8]

$$\mathbf{A} = \begin{pmatrix} 0 & 1 & 0 & \dots & 0 \\ 0 & 0 & 1 & \dots & 0 \\ \vdots & \vdots & \vdots & \ddots & \vdots \\ 0 & 0 & 0 & \dots & 1 \\ a_m & a_{m-1} & a_{m-2} & \dots & a_1 \end{pmatrix}_{m \times m},$$

$$\mathbf{B}^{(i)} = \begin{pmatrix} 0 \\ 0 \\ \vdots \\ 0 \\ b_i \end{pmatrix}_{m \times 1}, \quad (4)$$

where $i = 1, 2, \dots, m$.

It has been pointed out in the past [10] that it is undesirable to derive control laws based directly on Eq. (3). Following So and Ott [11], we introduce a $(2m-1)$ -dimensional expanded phase space, $\mathbf{Y}_n = (x_{n-m+1}, x_{n-m+2}, \dots, x_n, p_{n-m+1}, p_{n-m+2}, \dots, p_{n-1})^T$, to accommodate both dynamical measurements x_i and parameter changes p_i . In this expanded phase space, near the unstable fixed point $\mathbf{Y}^* = (x^*, \dots, x^*, p^*, \dots, p^*)^T$, the linearized dynamics becomes

$$\mathbf{Y}_{n+1} - \mathbf{Y}^* = \tilde{\mathbf{A}}(\mathbf{Y}_n - \mathbf{Y}^*) + \tilde{\mathbf{B}}(p_n - p^*), \quad (5)$$

with

$$\tilde{\mathbf{A}} = \begin{pmatrix} \mathbf{A} & \mathbf{B}^{(m)} & \mathbf{B}^{(m-1)} & \mathbf{B}^{(m-2)} & \dots & \mathbf{B}^{(2)} \\ \mathbf{0} & 0 & 1 & 0 & \dots & 0 \\ \mathbf{0} & 0 & 0 & 1 & \dots & 0 \\ \vdots & \vdots & \vdots & \vdots & \ddots & \vdots \\ \mathbf{0} & 0 & 0 & 0 & \dots & 1 \\ \mathbf{0} & 0 & 0 & 0 & \dots & 0 \end{pmatrix}_{(2m-1) \times (2m-1)}, \quad \tilde{\mathbf{B}} = \begin{pmatrix} \mathbf{B}^{(1)} \\ 0 \\ \vdots \\ 0 \\ 1 \end{pmatrix}_{(2m-1) \times 1}, \quad (6)$$

where $\mathbf{0}$ indicates an m -dimensional row vector of 0's.

To control, we apply a suitable perturbation $\delta p_n = p_n - p^*$, following each measurement x_n , to keep the dynamics within the stable subspace of $\tilde{\mathbf{A}}$. For a fixed point with u unstable directions, the control law governing the choice of δp_n is derived to be [8]

$$\delta p_n = - \left(\sum_{k=1}^u \frac{(\lambda_k)^u}{(\mathbf{v}_k^T \tilde{\mathbf{B}} \prod_{i=1, i \neq k}^u (\lambda_k - \lambda_i))} \mathbf{v}_k^T \right) \delta \mathbf{Y}_n, \quad (7)$$

where λ_k are the unstable eigenvalues of $\tilde{\mathbf{A}}$, ordered in descending absolute value, and the contravariant unstable eigenvectors \mathbf{v}_k are defined by $\tilde{\mathbf{A}}^T \mathbf{v}_k = \lambda_k \mathbf{v}_k$. It can be shown [8] that the elements of $\mathbf{v}_k = (v_k^{(1)}, v_k^{(2)}, \dots, v_k^{(2m-1)})$ are $v_k^{(i)} = \sum_{j=1}^i a_{m-j+1} (\lambda_k)^{j-i-1}$ for $i < m$, $v_k^m = 1$, and $v_k^{(i)} = \sum_{j=1}^{i-m} b_{m-j+1} (\lambda_k)^{j+m-i-1}$ for $i > m$.

Next, we consider the mechanism to update the above controller as the environment drifts over time. In terms of the measured variable x and the parameter p , from Eq. (3), we have

$$x_{n+1} - x^* = \sum_{\alpha=1}^m a_\alpha (x_{n-\alpha+1} - x^*) + \sum_{\beta=0}^m b_\beta \delta p_{n-\beta+1}. \quad (8)$$

The quantities a_α , b_β , and x^* in the above difference equation fully determine the control law in Eq. (7). In fact, a major step toward achieving initial control is to find ways to fit the unperturbed and perturbed dynamics near the fixed point to obtain the values of these parameters. This is usually done with the least-squares technique (see [8]). Here we suppose that this step has been completed. Assume now that the system parameters have changed slightly, such that the fixed point position and the shape of the linear region are modified, but not so much that the control is lost or that the dynamics during control are outside the linear region of the new fixed point. In this case, Eq. (8) still applies, and we can use a short history of N points incorporating the most recent measurements of the system state and perturbations to refit the control parameters. This refitting can be repeated as often as once per measurement cycle and requires no *a priori* knowledge or assumptions about how the environment has changed.

Below we explain how to update the fixed point position x^* and the parameter a 's and b 's in two separate steps, since each fitting step incorporates a different idea. In practice, these steps can be combined into one step.

(1) Assume that a 's and b 's remain constant for the duration of N iterates. From the expression in Eq. (8), we obtain

$$\begin{aligned} \langle x_{n+1} - x^* \rangle_N &= \sum_{\alpha=1}^m a_\alpha \langle x_{n-\alpha+1} - x^* \rangle_N \\ &+ \sum_{\beta=1}^m b_\beta \langle \delta p_{n-\beta+1} \rangle_N, \end{aligned} \quad (9)$$

where $\langle \rangle_N$ denotes average over the history of N measurements. Upon rearranging terms we have

$$x^* = \langle x_n \rangle_N + \frac{\sum_\beta b_\beta}{1 - \sum_\alpha a_\alpha} \langle \delta p_n \rangle_N = \langle x_n \rangle_N + g \langle \delta p_n \rangle_N, \quad (10)$$

where

$$g = \frac{\sum_\beta b_\beta}{1 - \sum_\alpha a_\alpha}. \quad (11)$$

At the end of this fitting cycle, $\langle x^* \rangle_N$ is taken as the new fixed point position. Although this method of calculating x^* may seem simplistic, by construction it guards against a nonzero average in δp . Therefore, its use maintains the small-perturbation quality of the control.

(2) Assuming now that x^* is a constant, from N iterates, we apply a least-squares fit to Eq. (8) to get the values of the a 's and b 's. To do so accurately, we must enforce a small amount of motion about the fixed point, because incessant applications of control suppress the motion around the fixed point, making the estimation of the a 's and b 's difficult. (This technique is called interrogation by Petrov *et al.* [7].) It is worthwhile to note that control can often be maintained for a while during the environment change without having to update the a 's and b 's. However, when the control fails as a result of the actual fixed point being too far removed from its original known location, it is often too late to update the a 's and b 's. By enforcing a small amount of natural local dynamics, we are able to update the a 's and b 's more precisely and more frequently. Specifically, this is done as follows. We monitor the absolute value of the perturbation δp_n . If it is smaller than some predetermined threshold δp_{\min} , we do not apply the perturbation (i.e., setting $\delta p_n = 0$) and let the system evolve freely for that iterate. This proves effective both in our numerical and experimental work.

The estimated values of x^* and a 's and b 's are subject to statistical fluctuations that can be very significant at times. As a precaution, we test the veracity of the newly derived parameters by checking whether the new values are close to the previous values [13]. In fitting x^* , we define a maximal distance between the newly estimated value and the previously used value. If the measured distance exceeds this maximal distance, we do not update the fixed point position. In testing both the a 's and the b 's we rely on quantities derived from a 's and b 's. Since the a 's describe the unperturbed dynamics near the unstable fixed point, the critical information they contain for control purposes is the directions of the stable and unstable manifolds of the fixed point. As a test of the fit of the a 's, we place a maximal angular deviation of, say, 15° between the new most unstable direction and the previous one. In order to test the new values of the b 's, we limit the fractional difference in the quantity g defined in Eq. (11). Specifically, in the experimental work reported in Sec. IV, we require

$$\frac{(g_{\text{calc}} - g_{\text{old}})^2}{|g_{\text{calc}}^* g_{\text{old}}|} < 2.25. \quad (12)$$

We comment, however, that for a given system one should tailor the criteria to achieve the best result.

III. NUMERICAL EXAMPLES

Now we apply the tracking technique above to three numerical examples chosen to illustrate various aspects of the technique: the Hénon map, a chemical reaction model, and a

coupled driven Duffing oscillator. For the Hénon map, all the parameters in the control law can be calculated exactly in terms of the original map parameters. Therefore, its study provides a way to check the fidelity of the parameter values estimated from time series using the procedure described in the preceding section. The chemical reaction model is an autonomous system. Here the observed discrete variable is the interval between successive crossings of some threshold by the system state. It has been shown [8,14] that these intervals, called interspike intervals, sample the dynamics of the original continuous time series on some Poincaré surface of section. Finally, the periodically driven coupled Duffing oscillator, probed at the integer multiples of the external driving period, is described by a four-dimensional discrete map. The key point here is that the periodic orbit to be stabilized and followed has two unstable directions.

A. The Hénon map: An analytically tractable example

The Hénon map is

$$x_{n+1} = p_n - x_n^2 + 0.3y_n, \quad y_{n+1} = x_n. \quad (13)$$

Here we use a subscript n to denote the time dependence of the parameter $p_n = p^* + \delta p_n$ during the course of control. Assuming that x is the observed scalar variable, from Eq. (13) this variable obeys the following second-order difference equation

$$x_{n+1} = p_n - x_n^2 + 0.3x_{n-1}. \quad (14)$$

Reconstructing the x time series in a two-dimensional space ($m=2$), we obtain the delay vector $\mathbf{z}_n = (z_n^{(1)}, z_n^{(2)}) = (x_{n-1}, x_n)$. From Eq. (14), the map \mathbf{G} for \mathbf{z}_n [see Eq. (2)] can be explicitly written as

$$\begin{pmatrix} z_{n+1}^{(1)} \\ z_{n+1}^{(2)} \end{pmatrix} = \begin{pmatrix} z_n^{(2)} \\ p_n - (z_n^{(2)})^2 + 0.3z_n^{(1)} \end{pmatrix}. \quad (15)$$

For $p_n = p^*$, the fixed point of interest is

$$x^* = (-0.7 + \sqrt{0.49 + 4p^*})/2. \quad (16)$$

Linearizing Eq. (15) about x^* leads to

$$\begin{pmatrix} \delta z_{n+1}^{(1)} \\ \delta z_{n+1}^{(2)} \end{pmatrix} = \begin{pmatrix} 0 & 1 \\ 0.3 & -2x^* \end{pmatrix} \begin{pmatrix} \delta z_n^{(1)} \\ \delta z_n^{(2)} \end{pmatrix} + \begin{pmatrix} 0 \\ 1 \end{pmatrix} \delta p_n. \quad (17)$$

From the above equation, we identify the parameters in the matrix \mathbf{A} and the vector $\mathbf{B}^{(i)}$ [see Eq. (3)] as $a_1 = -2x^* = 0.7 - \sqrt{0.49 + 4p^*}$, $a_2 = 0.3$, $b_1 = 1$, and $b_2 = 0$.

Let the parameter p^* vary over time as shown in Fig. 1(a). (Notice that in this case the varying parameter and the control parameter are the same.) Figure 1(b) shows the result of only updating the fixed point position without concurrently updating the a 's and b 's. It can be seen that the control can be maintained for a while, but it eventually fails when the fixed point is too far removed from its original location, where the a 's and b 's were initially obtained. Figure 1(c) shows the result of tracking the fixed point while updating both the a 's and b 's. Here we use a history of $N=20$ iterates in Eq. (10). If the analytically computed position of the fixed point, Eq. (16), is plotted as a function of time n , this plot coincides with the tracked position of the

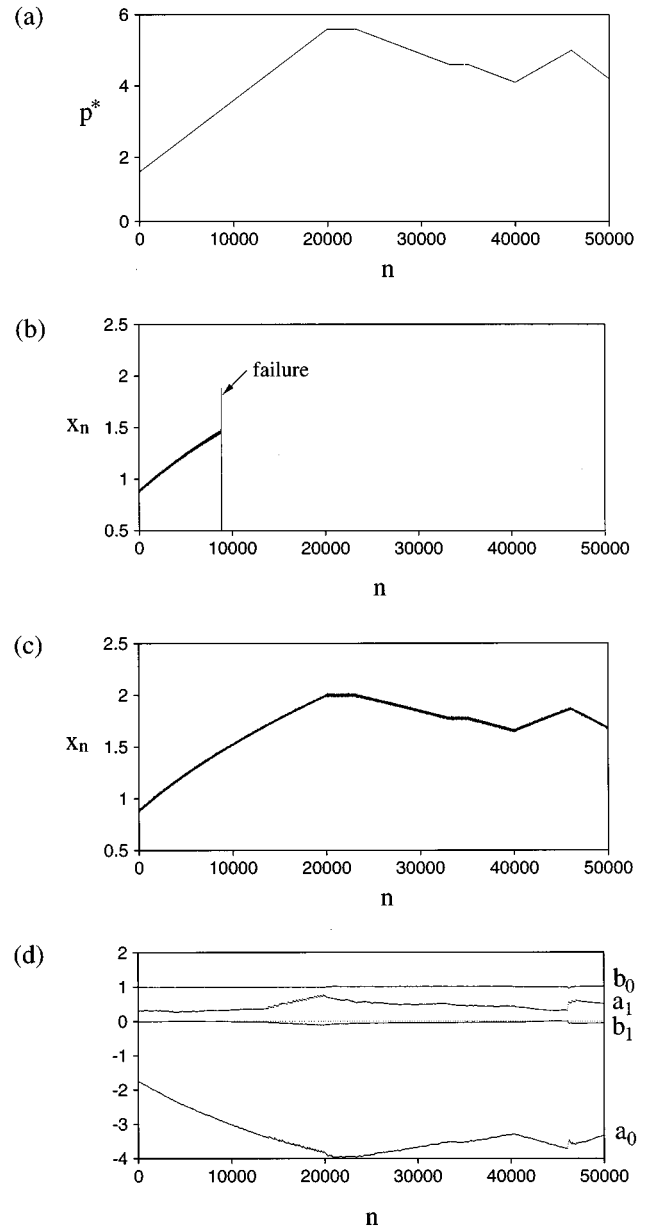


FIG. 1. (a) Slow variation of the nominal value p^* of the control parameter p as a function of the iterate n in the Hénon map, Eq. (13). (b) Result of updating only the fixed point position without concurrently updating the a 's and b 's. (c) Result of updating both the fixed point position and the a 's and b 's. (d) Estimated values of the a 's and b 's from the time series during control and tracking.

fixed point in Fig. 1(c). In addition, Fig. 1(d) shows the estimated values of a 's and b 's from the time series $\{x_n\}$. These estimated values agree well with their actual analytical values, given earlier. These results demonstrate that the control and tracking procedure outlined in the preceding section works effectively for the Hénon map.

B. A chemical reaction model: Tracking and control using interspike intervals

In experimental problems, we expect to encounter two kinds of continuous time systems, autonomous and periodi-

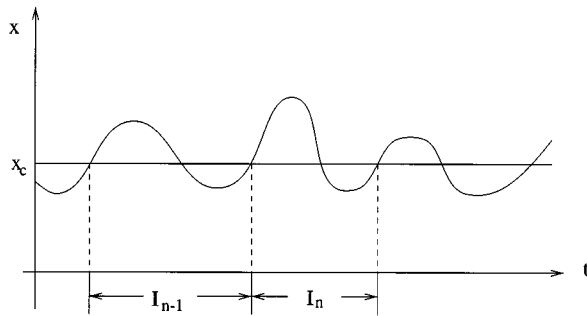


FIG. 2. Schematic illustration of the formation of interspike intervals $\{I_n\}$ from a continuous time series.

cally driven. For a periodically driven system, a discrete Poincaré map can be formed by sampling the dynamics at every period of the driving. We will show an example of how to control and track unstable periodic orbits in such systems in the next subsection. In the present subsection we introduce a technique to form a discrete Poincaré-map-generated time series for autonomous systems.

Consider the schematic in Fig. 2, where a scalar variable of the system state x is plotted against time. Choose a proper threshold $x = x_c$. We measure the intervals between successive crossings of the threshold by $x(t)$ from a given direction (upward crossing in the figure). This time series $\{I_n\}$, called

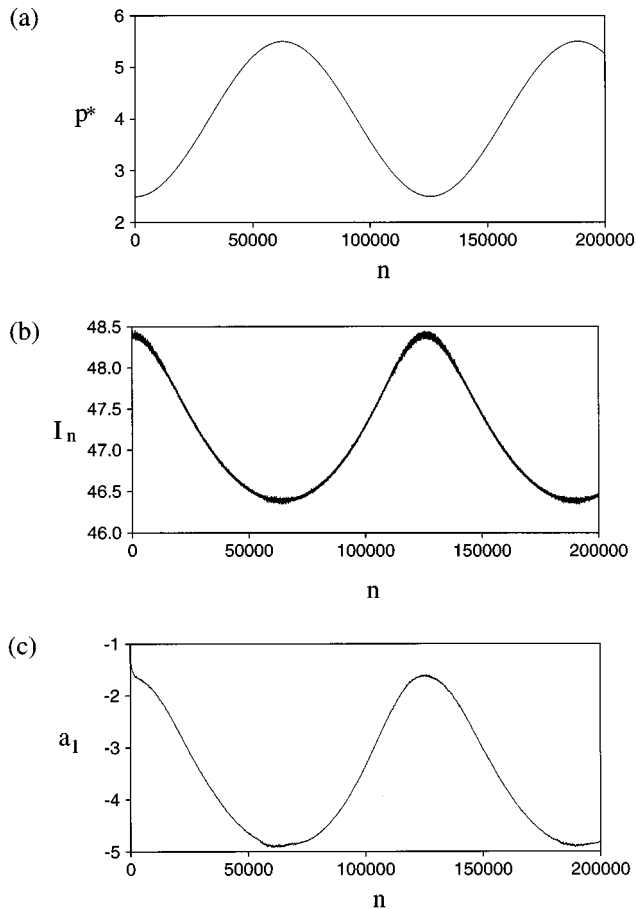


FIG. 3. (a) Slow variation of the nominal value p^* of the control parameter p in Eq. (18). (b) Measured interspike intervals during control and tracking. (c) Estimated value of a_1 during control and tracking.

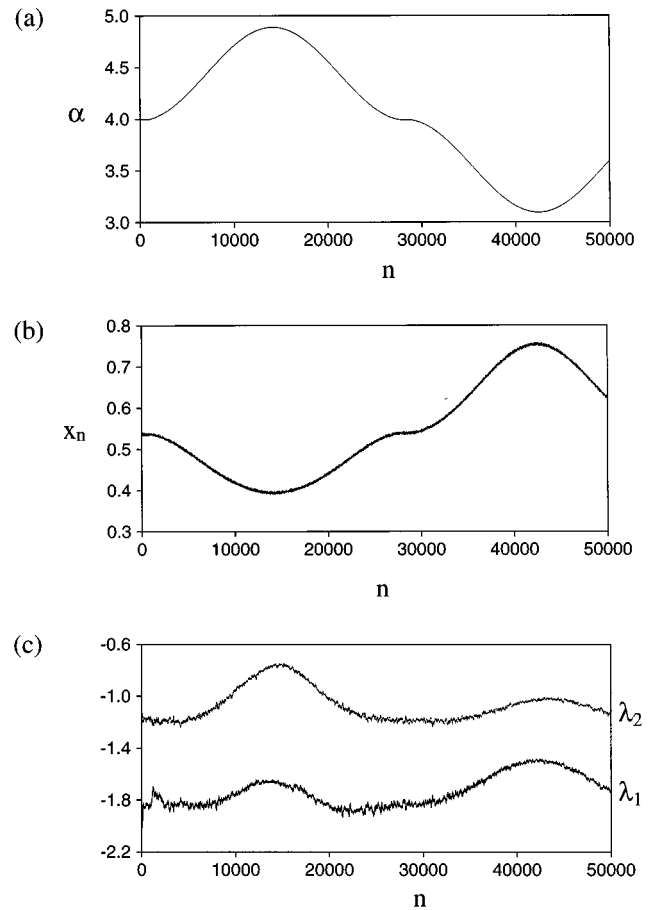


FIG. 4. (a) Slow drift of the parameter α in the coupled Duffing oscillator, Eq. (19). (b) Measured variable $x = x_1 + x_2$ during control and tracking. (c) First two eigenvalues of the fixed point during control and tracking.

interspike intervals, is shown [8,14] to sample the dynamics of the original continuous time dynamical system on some Poincaré surface of section and will be the time series we use below for control and tracking.

The example we consider here is the following four-dimensional chemical reaction model [15],

$$\dot{x} = pw/(1+w^{10}) - 0.1x, \quad \dot{y} = 0.1x - 0.2yz, \quad (18)$$

$$\dot{z} = 0.2z(y-w), \quad \dot{w} = 0.2zw - 0.1w.$$

When $p = p^* = 2.5$, this system exhibits a chaotic attractor. Assume that the observed scalar variable is x itself and p is the control parameter. By measuring the times between successive upward crossings of the threshold $x_c = 1$ by the x versus t function, we form the interspike interval time series $\{I_n\}$. The reconstructed attractor in an $(m=3)$ -dimensional delay-coordinate space has a dimension of 1.2 and contains a fixed point at $\mathbf{z}_n = (48.40, 48.40, 48.40)^T$. The stabilization of this fixed point is done in [8]. Now we consider the tracking of the fixed point when the nominal value of the parameter p , p^* drifts over time as shown in Fig. 3(a). Figure 3(b) shows the result of applying the tracking procedure of Sec. II. The estimated value of a_1 is shown in Fig. 3(c). Here we use $N=20$ in Eq. (10) for updating both the fixed point po-

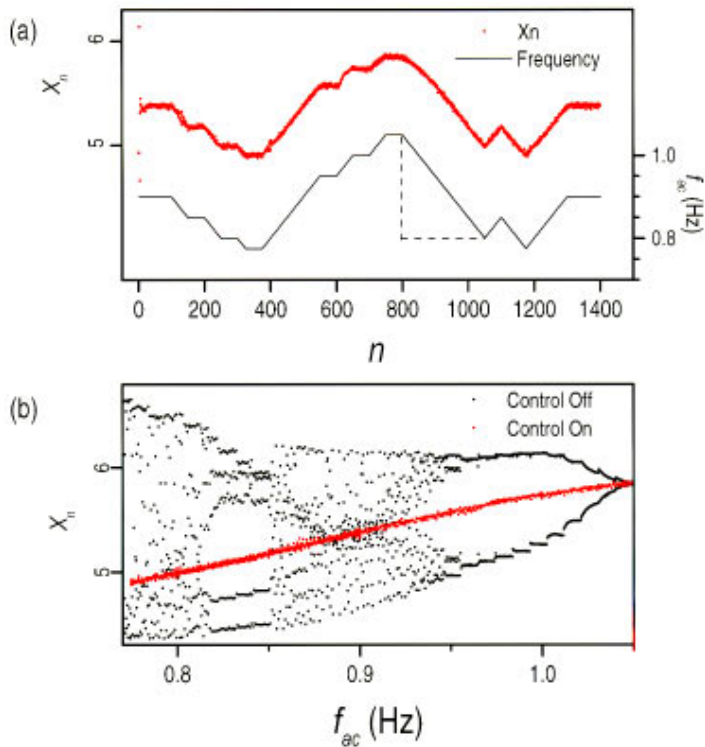


FIG. 5. (Color) (a) Measured ribbon position (red dots) during control and tracking as a function of iteration n in the presence of a time-varying drive frequency f_{ac} (solid black line). Note that once control was established it was never lost, despite relatively fast variations of f_{ac} . The dotted lines indicate a total change in frequency of 0.25 Hz in 250 iterations, a rate greater than 1% per iteration. (b) Same ribbon position data (red dots) as in (a) superposed on the bifurcation diagram (black dots) of the uncontrolled system.

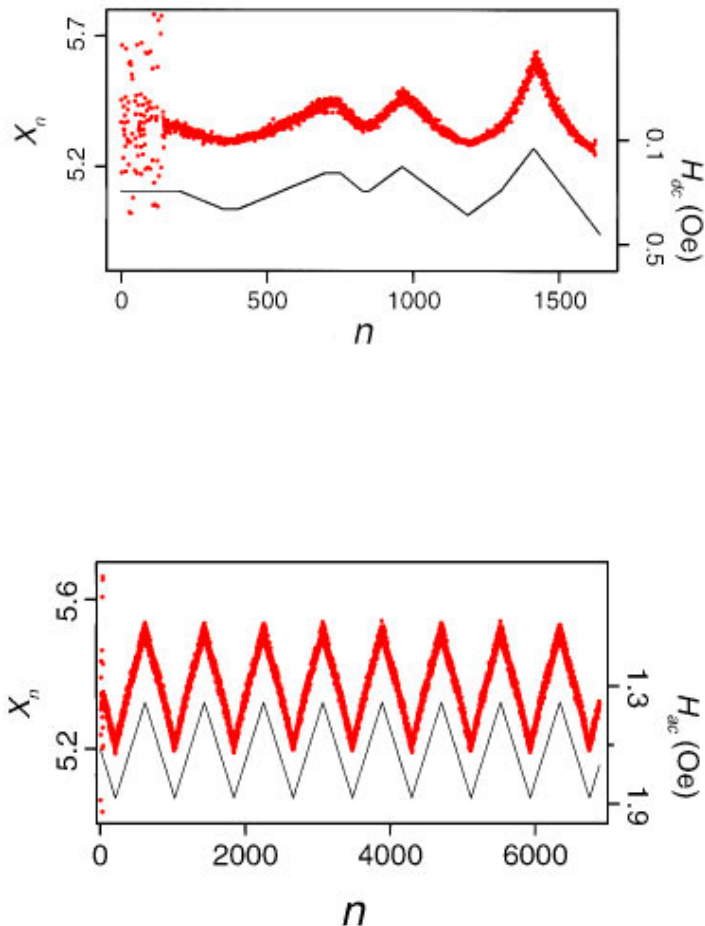


FIG. 6. (Color) Measured ribbon position (red dots) during control and tracking as a function of iteration n in the presence of a time-varying dc magnetic field H_{dc} (solid black line). Note that control was not turned on until after iteration $n = 150$.

FIG. 7. (Color) Measured ribbon position (red dots) during control and tracking as a function of iteration n in the presence of a time-varying ac magnetic field H_{ac} (solid black line).

sition and the a 's and b 's. Evidently, we are able to maintain control during the course of environmental drift. Although we do not have analytical results with which to compare the numerical results, we can still see quite clearly that the tracked fixed point and a_1 follow the trend in the variation of p^* .

C. Coupled driven Duffing oscillator: Tracking fixed point with multiple unstable directions

Consider the following five-dimensional system of two coupled driven Duffing oscillators:

$$\ddot{x}_1 + \gamma\dot{x}_1 + \alpha(x_1^3 - x_1) + \beta_1(x_1 - x_2) = p_1 \sin(\omega t), \quad (19)$$

$$\ddot{x}_2 + \gamma\dot{x}_2 + \alpha(x_2^3 - x_2) + \beta_2(x_2 - x_1) = p \sin(\omega t).$$

For $\gamma=0.632$, $\alpha=4.0$, $\beta_1=0.1$, $\beta_2=0.05$, $\omega=2.1235$, $p_1=1.011$, and $p=p^*=p_1$, Eq. (19) exhibits a chaotic attractor of dimension $D=3.3$. The scalar observable here is $x=x_1+x_2$ and we sample the attractor every cycle of the external forcing. The attractor, reconstructed using the time series $\{x_n\}$ in an ($m=4$)-dimensional delay-coordinates space, has a dimension $D=2.3$.

The reconstructed attractor contains a fixed point at $(0.54, 0.54, 0.54, 0.54)^T$. This fixed point corresponds to the synchronized period-one motion of the coupled oscillators and has two unstable directions ($u=2$). This orbit was originally stabilized in [8] using Eq. (7) with $m=4$. Now we let the environment, represented by the value of α , drift slowly over time, as shown in Fig. 4(a). With p as the control parameter, we attempt to maintain control by applying the adaptive control strategy developed earlier. The position of the tracked fixed point is shown in Fig. 4(b). Here we use $N=20$ in Eq. (10) for updating both the fixed point position and the a 's and b 's. Again, although the theoretical value of the fixed point position is not known, it is clear from the figure that its movement is compatible with the movement of α . Figure 4(c) show the values of the first two eigenvalues of the tracked fixed point. For the most part, both eigenvalues have magnitudes greater than one.

IV. PHYSICAL EXPERIMENT: THE MAGNETOELASTIC RIBBON

We have implemented and tested our tracking algorithm in a magnetoelastic ribbon system. This system, described in detail in [16], consists of a gravitationally buckled, amorphous magnetoelastic ribbon whose Young's modulus varies by as much as a factor of 10 as a function of the applied magnetic field parallel to its long axis. The ribbon is clamped vertically and its deflection from the vertical is measured optically near its base as the vertical magnetic field $H_z(t) = H_{dc} + H_{ac} \sin(2\pi f_{ac} t)$ is varied. The position x_n is then recorded stroboscopically at a constant phase of the sinusoidal drive. Control perturbations are applied in the form of small offsets to H_{dc} once per drive cycle, as computed from Eq. (7). To test the effectiveness and versatility of our adaptive control technique, we have made each of the three system parameters, H_{dc} , H_{ac} , or f_{ac} , slowly time dependent, where "slow" is relative to one drive period. No

information about how these parameters drift is used in the control algorithm.

The chaotic attractor, when driven with static parameters, requires three dimensions in delay coordinates ($m=3$) to fully unfold. As the parameters slowly drift, the attractor translates and bends. The fixed point to be controlled and tracked has one unstable and two stable directions. In each case, the recalculation of the control parameters was based on a history of $N=14$ previous measurements and applied perturbations.

The first case of tracking with our adaptive control technique is shown for a time varying f_{ac} in Fig. 5(a) (black line). We note that, because the measurement was done at a constant *phase* of the drive, the Poincaré map is constructed properly and consistently, despite changes in the frequency. This would not be the case if measurements were simply performed at a fixed constant interval. The measured ribbon position (red dots) is shown in Fig. 5(a) as a function of iteration n . As mentioned earlier, we use $N=14$ in Eq. (10) for updating the fixed point position and the a 's and b 's. Figure 5(b) shows the tracked fixed point position [same data set as in Fig. 5(a)] superposed on the natural, uncontrolled bifurcation diagram for the same range of f_{ac} variations.

Although we have no analytic confirmation that the computed fixed point position and control parameters correspond to those at constant drive parameter, two aspects of Fig. 5(b) yield secondary confirmation. First, from Fig. 5(b) we see that the unstable fixed point we controlled and tracked is the same orbit that became unstable through a period-doubling bifurcation at about $f_{ac}=1.05$. It is known theoretically that this orbit often mediates the merging of two chaotic bands into one chaotic band. The behavior of the tracked orbit is consistent with this theoretical observation in Fig. 5(b), indicating that the result of our tracking algorithm is indeed the fixed point. A second confirmation is that the tracked orbit in Fig. 5(b) follows one continuous line as a function of f_{ac} , despite the fact that it represents multiple passes through the same position in parameter space. This indicates that we are tracking the same fixed point, independent of history.

An equal degree of success was found in adapting to substantial variations in both H_{dc} and H_{ac} as drifting parameters, demonstrated in Figs. 6 and 7.

V. CONCLUSION

We have developed and experimentally implemented an adaptive control algorithm for maintaining control while the physical environment in which the system is situated varies slowly with time. The technique is an extension of the generalized high-dimensional control algorithm of Ding *et al.* [8]. Updated control parameters are derived while control is maintained and are based solely on recent short histories of the dynamics during control and the perturbations used to maintain control.

ACKNOWLEDGMENTS

This work was supported by the Office of Naval Research, Physical Sciences Division. B.G. was supported through the Office of Naval Research Postdoctoral Program. M.D.'s research is also supported by a grant from the National Institute of Mental Health to the Center for Complex Systems, Florida Atlantic University.

- [1] E. Ott, C. Grebogi, and J.A. Yorke, Phys. Rev. Lett. **64**, 1196 (1990).
- [2] For reviews, see T.A. Shinbrot, C. Grebogi, E. Ott, and J.A. Yorke, Nature (London) **363**, 411 (1993); W.L. Ditto and L.M. Pecora, Sci. Am. **269**, 78 (1993); G. Chen and X. Dong, Int. J. Bifur. Chaos **3**, 1363 (1993); E.R. Hunt and G. Johnson, IEEE Spectrum **30**, 32 (1993); R. Roy, Z. Gills, and K.S. Thornburg, Opt. Photon. News **5**, 8 (1994); E. Ott and M.L. Spano, Phys. Today **48** (5), 34 (1995).
- [3] B. Hunt and E. Ott, Phys. Rev. Lett. **76**, 2254 (1996).
- [4] M. Ding, E. Ott, and C. Grebogi, Physica D **74**, 386 (1994); Phys. Rev. E **50**, 4228 (1994); E.H. Abed, H.O. Wang, and R.C. Chen, Physica D **70**, 154 (1994).
- [5] I.B. Schwartz and I. Triandaf, Phys. Rev. A **46**, 7439 (1992).
- [6] T.L. Carroll, I. Triandaf, I.B. Schwartz, and L.M. Pecora, Phys. Rev. A **46**, 6189 (1992); Z. Gills, C. Iwata, R. Roy, I.B. Schwartz, and I. Triandaf, Phys. Rev. Lett. **69**, 3169 (1992); I. Triandaf and I.B. Schwartz, Phys. Rev. E **48**, 718 (1993); S. Bielawski, M. Bouazaoui, D. Derozier, and P. Glorieux, Phys. Rev. A **47**, 3276 (1993); N.F. Rulkov, L.S. Tsimring, and H.D.I. Abarbanel, Phys. Rev. E **50**, 314 (1994); V. Petrov, M.J. Crowley, and K. Showalter, Phys. Rev. Lett. **72**, 2955 (1994); V. In, W.L. Ditto, and M.L. Spano, Phys. Rev. E **51**, R2689 (1995); U. Dressler, T. Ritz, A. Schenck zu Schweinsberg, R. Doerner, B. Hübinger, and W. Martienssen, Phys. Rev. E **51**, 1845 (1995); K. Konishi and H. Kokame, Phys. Lett. A **206**, 203 (1995).
- [7] V. Petrov, S. Metens, P. Borckmans, G. Dewel, and K. Showalter, Phys. Rev. Lett. **75**, 2895 (1995).
- [8] M. Ding, W. Yang, V. In, W.L. Ditto, M.L. Spano, and B. Gluckman, Phys. Rev. E **53**, 4334 (1996).
- [9] F. Takens, in *Dynamical Systems and Turbulence*, edited by D. Rand and L.S. Young (Springer-Verlag, Berlin, 1981), p. 230; N.H. Packard, J.P. Crutchfield, J.D. Farmer, and R.S. Shaw, Phys. Rev. Lett. **45**, 712 (1980); J. P. Eckmann and D. Ruelle, Rev. Mod. Phys. **57**, 617 (1985).
- [10] U. Dressler and G. Nitsche, Phys. Rev. Lett. **68**, 1 (1992); G. Nitsche and U. Dressler, Physica D **58**, 153 (1992).
- [11] P. So and E. Ott, Phys. Rev. E **51**, 2955 (1995).
- [12] V. Petrov, E. Mihaliuk, S.K. Scott, and K. Showalter, Phys. Rev. E **51**, 3988 (1995).
- [13] The tests presented are simply one method for dealing with these statistical fluctuations, and are meant to eliminate the abnormally large fluctuations. Another method that we have successfully used is to update the control parameters to a value somewhere between the current value and computed value. For example, $x_{\text{new}}^* = 0.9x_{\text{old}}^* + 0.1x_{\text{calc}}^*$. This type of updating tends to add an additional delay in the response time of the control, but also minimizes oscillations in the estimated control parameters.
- [14] M. Ding and W. Yang, Phys. Rev. E **55**, 2397 (1997).
- [15] G. Baier and S. Sahle, J. Chem. Phys. **100**, 8907 (1994).
- [16] W.L. Ditto, S. Rauseo, R. Cawley, C. Grebogi, G.H. Hsu, E. Kostelich, E. Ott, H.T. Savage, R. Segnan, M.L. Spano, and J.A. Yorke, Phys. Rev. Lett. **63**, 923 (1989).